

Cooperative domains define a unique host cell-targeting signal in *Plasmodium falciparum*-infected erythrocytes

Carlos Lopez-Estraño, Souvik Bhattacharjee, Travis Harrison, and Kasturi Haldar*

Departments of Pathology and Microbiology–Immunology, The Feinberg School of Medicine, Northwestern University, Chicago, IL 60611

Edited by John J. Mekalanos, Harvard Medical School, Boston, MA, and approved August 19, 2003 (received for review May 21, 2003)

When the malaria parasite *Plasmodium falciparum* infects an erythrocyte, it resides in a parasitophorous vacuole and remarkably exports proteins into the periphery of its host cell. Two of these proteins, the histidine-rich proteins I and II (PfHRPI and PfHRPII), are exported to the erythrocyte cytoplasm. PfHRPI has been linked to cell-surface “knobby” protrusions that mediate cerebral malaria and are a frequent cause of death. PfHRPII has been implicated in (i) the production of hemozoin, the black pigment associated with disease, as well as (ii) interactions with the erythrocyte cytoskeleton. Here we show that a tripartite signal that is comprised of an endoplasmic reticulum-type signal sequence followed by a bipartite vacuolar translocation signal derived from HRPII and HRPI exports GFP from the parasitophorous vacuole to the host cytoplasm. The bipartite vacuolar translocation signal is comprised of unique, peptidic (≈40-aa) sequences. A domain within it contains the signal for export to “cleft” transport intermediates in the host erythrocyte and may thereby regulate the pathway of export to the host cytoplasm. A signal for posttranslational, vacuolar exit of proteins has hitherto not been described in eukaryotic secretion.

Mature erythrocytes are terminally differentiated, devoid of all intracellular organelles, incapable of *de novo* protein or lipid synthesis, and lack endocytic machinery (1, 2). However, they can be infected by the parasite *Plasmodium falciparum* (3, 4), which causes the most virulent form of human malaria, a disease that afflicts 200–300 million people and kills 1–2 million children a year (5, 6). The blood stages of *P. falciparum* that infect erythrocytes are responsible for all the pathologies and symptoms associated with the disease. Proteins synthesized by the parasite and exported to the mature erythrocyte induce profound antigenic and structural changes in the cytosol and membrane of this enucleated host cell (7, 8).

Prominent among exported parasite proteins are the *P. falciparum* histidine-rich proteins I (9) and II (10) (PfHRPI and PfHRPII). PfHRPI is a major constituent protein of “knobs”: these are electron-dense structures protruding upward from the host skeleton that are important for adhesion of infected erythrocytes to endothelial cells in cerebral malaria (11). PfHRPII has been implicated as a heme polymerase (12) that catalyzes the formation of hemozoin (13), the black pigment associated with numerous pathologies of severe malaria (14–16). More recent studies suggest that it may function as an actin-binding protein (17). Similar to PfHRPI, PfHRPII is also delivered to the cytoplasm in the periphery of the red cell (18). However, how these and other parasite proteins move from the vacuolar parasite to the periphery of the erythrocyte in the absence of endogenous host, cytosolic transport machinery, remains an enigma.

A few studies have suggested that components of vesicular sorting machinery such as Sar1p, *N*-ethylmaleimide-sensitive factor, and Sec31 are exported from within the cytosol of the parasite to intraerythrocytic structures called the Maurer’s clefts (19–21), but functional evidence for this is still lacking. Moreover, although several proteins exported to the erythrocyte cytosol have been detected in association with clefts (22–24),

how these organelles are targeted is not known. Studies on signals required for protein export show that an N-terminal endoplasmic reticulum (ER)-type signal sequence (SS) transports protein to the parasitophorous vacuole (PV) (24–27). This seems to be a conserved property of SS detected in several malarial antigens (8) and likely reflects default secretion to the plasma membrane expected in a eukaryotic cell. Notably, the signals that underlie critical targeting of proteins from the PV to the red cell and molecular evidence of their function in export have remained elusive. It has been argued in the case of PfHRPI (and presumably other HRPs) that the export signals must reside in non-histidine-rich sequences of histidine-rich domains (24), because many parasite proteins exported to the erythrocyte are not histidine-rich.

In this study we used sequences derived from PfHRPII and PfHRPI. We show that previously uncharacterized ≈40-aa bipartite peptidic signals comprised of a minimal histidine-rich sequence 9–13 amino acids from the histidine domain II and domain I containing 26–29 amino acids that reside between the SS and the histidine-rich domain II of these proteins (Fig. 1) are necessary and sufficient for protein export from the PV to the erythrocyte cytosol. These peptides define peptidic vacuolar translocation signals (VTSs) for a eukaryotic pathogen that resides in an intracellular vacuole. On its own, domain II (or a minimal histidine sequence from within it) can export GFP to intraerythrocytic structures called the Maurer’s clefts but does not mediate protein release into the erythrocyte cytoplasm. The latter step requires a cooperative signal assembled from both domain I and II in the VTS. It is interesting to note that histidines can be substituted by arginines, suggesting a requirement for charge in this posttranslational, signal-mediated protein exit from vacuolar intraerythrocytic organelles. The results are discussed in the context of VTS-associated models of PV-cleft export secretion systems.

Materials and Methods

Plasmid Constructs and Transgene Expression. All constructs used for transfections are listed in Table 1 (which is published as supporting information on the PNAS web site, www.pnas.org) in the order that they appear in *Results*. PfHRPIIGFP expression was obtained by transfecting cells with the plasmid pDCHRPI-IGFP. This plasmid was constructed as follows. HRPIImyc (18) was cloned into the *Xho*I site in pBluescript SK(+) (Stratagene) to generate pBSHRPIImyc. A unique *Bgl*II site was located between the end of the HRPII coding region and the myc tag on the pBSHRPIImyc plasmid. Into this site we inserted a *Bgl*II–

This paper was submitted directly (Track II) to the PNAS office.

Abbreviations: Pf, *Plasmodium falciparum*; HRPI and HRPII, histidine-rich proteins I and II, respectively; ER, endoplasmic reticulum; SS, signal sequence; PV, parasitophorous vacuole; VTS, vacuolar translocation signal.

*To whom correspondence should be addressed at: Department of Pathology, Ward Building, Room 3-240, The Feinberg School of Medicine, Northwestern University, 303 Chicago Avenue, Chicago, IL 60611. E-mail: k-haldar@northwestern.edu.

© 2003 by The National Academy of Sciences of the USA



Fig. 1. Structure of PfHRPII and PfHRPI and expression of transgenes. (A*i*) PfHRPII protein sequence (44) contains a cleavable, ER-type signal peptide (shown in orange) as predicted by Signal P. An asparagine-rich region called domain I (shown in black) is followed by a histidine-rich C-terminal domain (II, shown in pink). Subscript numbers indicate truncations used in GFP constructs. (A*ii*) For PfHRPI (9), sequences for the ER-type signal (lowercase), domain I (gray), and the first histidine region (II, amino acids 61–106, in blue) are shown. (B) Western blot analysis of total infected cell lysates containing fusion proteins PfHRPIIGFP (lane i), SSHRPIIDomainIGFP (lane ii), SSGFP (lane iii), SSHRPIIDomainIHis.reg.57–124 GFP (lane iv), SSHRPIIDomainIHis.minGFP (lane v), GFPHis.reg.154–327 (lane vi), and SSGFPHis.reg.154–327 (lane vii) and probed with antibodies to GFP. Arrowheads indicate the expected fusion protein. Arrows indicate predicted unprocessed secretory precursors. Some constructs showed low levels of degradation product that migrated at the predicted size of GFP (asterisk). Molecular mass (in kDa) is shown on the left side of each blot.

*Bam*HI GFP fragment derived from pHRPGFP (28) to generate pBSHRPIIGFP, which was subsequently cloned into the pDC1 (29) *Xho*I site. Assembly in pBluescript SK(+) and subcloning into pDC were adopted for all constructs. pDCSSHRPII-DomainIGFP was constructed as follows. SSHRPIIDomainI was amplified from pBSHRPIImyc by PCR with the primers 5'-CTATCTAGACTCGAGATGCATAGATCTAAAGGAG-AAGAACTTTTC-3' and 5'-ATCAGATCTGACGTCATCATGTGCTTGAGTTTCGTATAATAATC-3' (underlined sequences indicate restriction sites for cloning, boldfaced sequences indicate internal restriction sites) carrying *Xba*I at the 5' end and *Bgl*II at the 3' end. This fragment was cloned into pBSHRPIIGFP digested with *Bgl*II and *Xba*I to generate SSHRPIIDomainIGFP, which was subsequently cloned into pDC. pDCSSGFP was constructed as follows. The SS of PfHRPII was amplified by PCR with the primers 5'-ATCCTGACGCTCGAGATGGTTTCTCTCAAAAATAAAGTATTATCC-3' and 5'-ATCAGATCTTGCTGCGGCTGCACACAAGT-TATTATAAATGCGGAATTATTC-3' and cloned into pBSHRPIIGFP digested with *Pst*I and *Bgl*III. This resulted in replacing HRPII with SS to generate SSGFP, which was subcloned into pDC1. pDCSSHRPIIDomainIHis.reg.57–124GFP was constructed by digesting the plasmid pBSHRPIImyc with *Nsi*I and *Xho*I. The resulting fragment containing SSDomainIHis.reg.57–124 was cloned in frame into pBSHRPIIGFP and then subcloned into pDC1. pDCSSHRPIIDomainIHis.min.GFP was constructed as follows. We created in SSHRPIIDomainIGFP an *Aat*II site at the end of the SSHRPIIDomainI sequence just before the *Bgl*II site. This enabled insertion of a minimal histidine domain that was generated by complementary oligonucleotides 5'-CTCGACGTCATCATGCTCATCATGC-CGACGTCCTC-3' and 5'-GAGACGTCGGCATGATGAG-CATGATGGACGTCGAG-3' carrying an *Aat*II restriction site. This gave rise to pBSSSHRPIIDomainIHis.min.GFP, which was cloned into pDC1. The minimal histidine peptide was selected for its conservation of four histidines seen in the C-terminal repeats of HRPII. To design required restriction sites we allowed for loss of a single valine 63 and conserved substitutions replacing valine for alanine and vice versa. pDCGFPHis.reg.154–327 was constructed as follows. The terminal histidine-rich domain (amino acids 154–327) of HRP II was obtained by digesting HRPIImyc with *Nsi*I and *Xho*I. The resulting fragment was cloned into pBluescript digested with *Xho*I and *Pst*I. This insertion was out of frame. To correct for frame in the final construct, GFP was amplified by PCR from the pHRPGFP (28) by using the primers

5'-CTATCTAGACTCGAGATGCATAGATCTAAAGGA-GAAGAACTTTTC-3' and 5'-TGAGGATCCCTGCTGCTGCTGCTTTGTATAGTTCATCCATGCCATGTGTAATCC-C-3' and inserted upstream of the histidine sequence to generate GFPHis.reg.154–327. To construct pDCSSGFPHis.reg.154–327, the SS was inserted by cloning into pBSGFPHis.reg.154–327 digested with *Pst*I and *Bgl*III to generate pBSSSGFPHis.reg.154–327. Subsequent cloning into pDC1 generated pDCSSGFPHis.reg.154–327. pDCSSHRPIIDomainIHis.reg.57–124GFP was constructed as follows. The ΔDomainI region of PfHRPII domain I was generated by PCR mutagenesis. The forward primer used was 5'-ATCAGATCTAATAAGAGATTATTATACGAAAC-TCAAGC-3', which spans the sequence between amino acids 43 and 51. The reverse primer at the GFP 3' end was 5'-ATCGGTACCCTCGAGTTTGTATAGTTCATCCATGCCATGTGTAATC-3'; as template we used SSHRPIIDomainIHis.reg.57–124GFP. The resulting product was digested with *Bgl*III and *Kpn*I and inserted into pBSSSGFP digested with *Bgl*III and *Kpn*I to generate SSHRPIIDomainIHis.reg.57–124GFP, which was subsequently cloned into pDC1. pDCSSGFPHRPII-DomainIHis.min was made by first subcloning a GFP fragment obtained by digesting pHRPGFP (28) with *Nsi*I and *Hind*III into pBluescript digested with *Pst*I and *Hind*III. SS was obtained by *Xba*I–*Bgl*III digestion of SSGFP and was subsequently inserted to generate SSGFP', which resulted in abrogation of a *Bam*HI site in the fragment SS–*Xba*I–*Bgl*III. The minimal histidine repeat was generated by complementary oligonucleotides 5'-CTCGGATCCGACGTCATCATGCTCATCATGCCGACGTCAGATCTCTC-3' and 5'-GAGAGATCTGACGTCG-GCATGATGAGCATGATGGACGTCGGATCCGAG-3', and the resulting fragment was inserted into the *Bam*HI site at the very C terminus of GFP to give rise to SSGFPHis.min. This was digested with *Bam*HI, and a PCR fragment of the HRPIIDomain I region (5'-ATCAGATCTGCATTTAATAAATAACTTGTGTAGCAAAAATGC-3' and 5'-ATCAGATCTGACGTCATCTACATGTGCTTGAGTTTCGTATAATAATC-3') was inserted to generate pBSSSGFPHRPIIDomainIHis.min, which was subsequently cloned into pDC1. pDCSSHRPII-DomainIGFPHis.reg.154–327 was generated by digestion of pBSSSHRPIIDomainIGFP with *Xba*I–*Bgl*III to produce a fragment containing SSHRPIIDomainI. This fragment was cloned into pBSGFPHis.reg.157–327 digested with *Xba*I and *Bgl*III. The SSHRPIIDomainIGFPHis.reg.154–327 was subsequently cloned into pDC1.

In pDCHRPIDomainIGFP, the PfHRPI (KAHRP) domain I

was synthesized with two self-annealing oligonucleotides, 5'-CATGGATCCTCTAATAATTGCAATAATGGAAACGGATCTGGTGACTCCTTCGATTTTCAGA-3' and 5'-TAGAGATCTTTGCTTTTGTGCTAAAGTTCTCTTATTTCTGAAATCGAAGGAGTCCACCAGA-3', extended by using Klenow (NEB) and inserted in pBSSSGFP to generate pBSSSHRPIIDomainIGFP. (Note that, in chimeric sequences, all HRPI sequences are shown in bold type and HRPII sequences are shown in bold and italic type). We then inserted the HRPIIHis.min sequence, VHHAHHADV, into SSHRPI-DomainIGFP and generated pBSSSHRPIIDomainIHRPIIHis.min.GFP, which was subsequently cloned into pDC1 to give rise to pDCSSHRPIIDomainIHRPIIHis.min.

pDCSSHRPIIDomainIHRPIIHis.minGFP was constructed as follows. A minimal HRPI histidine-rich region of 13 histidine residues, which resembles the first histidine stretch in the native HRPI, was generated by the complementary oligonucleotides 5'-ATCAGATCTCATGAACACCATCACCACCATCAC-CATC-3' and 5'-ATCAGATCTATGATGGTGGTGGTGGTGGTGGTGGTGG-3'. The fragment was cloned into pBSSS-DomainIGFP to generate SSHRPIIDomainIHRPIIHis.minGFP, which was cloned into pDC1. Arginine substitutions leading to pDCSSHRPIIDomainIArg.minGFP were generated by the complementary oligonucleotides 5'-CTCGACGTCAGGAG-GCTAGGAGGGCCGACGTCCTC-3' and 5'-GAGGACGTCGGCCCTCCTAGCCCTCCTGACGTCGAG-3'. The fragment was inserted into a *Bgl*II site in pBSSSHRPIIDomainIGFP, giving rise to SSHRPIIDomainIArg.minGFP, which was subsequently subcloned into pDC1.

P. falciparum-infected erythrocytes (3D7 strain) were transfected as described (29, 30). Forty-eight hours after transfection, methotrexate (Sigma) was added to the culture medium and maintained at a concentration of 1.3 μ M until the cell lines were established (3–4 weeks). Drug concentrations (1–10 μ M final concentration) were increased periodically until 90% of the parasite population expressed GFP. The transgenic *P. falciparum* cell lines were subsequently grown *in vitro* under standard culture conditions.

Cell Permeabilization, Fluorescence Microscopy, and Indirect Immunofluorescence Assays. Infected red cells at 15–20% parasitemia and 2.5% hematocrit were incubated with 100 units of tetanolysin (hemolytic units were described by the manufacturer, List Biological Laboratories, Campbell, CA) for 50 min at 37°C. The permeabilized preparations were subjected to centrifugation at 2,200 \times *g* for 10 min, and the resulting pellet and supernatant fractions were examined in Western blots. For microscopy studies, cell preparations for both live and fixed cells were carried out essentially as described (25). Briefly, in indirect immunofluorescence assays, cells were fixed in 1–2% formaldehyde, permeabilized with 0.05% saponin, blocked with 0.2% fish-skin gelatin, probed with antibodies to GFP (Molecular Probes, no. A6455) and/or LWL1 (31) (an antibody to the major resident protein of Maurer's clefts), and then incubated with the appropriate secondary antibodies in PBS containing 0.2% fish-skin gelatin. For all cells, parasite nuclei were stained with 10 μ g/ml Hoechst for 5 min. Fluorescence microscopy and digital-image collection were performed on an Olympus (New Hyde Park, NY) IX inverted fluorescence microscope and a Photometrix (Tucson, AZ) cooled charge-coupled device camera (CH350/LCCD) driven by DELTAVISION software from Applied Precision (Seattle).

Results

A Minimal Histidine-Rich Domain and Domain I of PfHRPII Constitute a Peptidic VTS That Targets GFP from the PV to the Erythrocyte Cytoplasm. We have shown previously that a tagged transgene PfHRPII_{myc} can be expressed and exported to the host red cell

(18). To study the trafficking of PfHRPII in live cells we expressed a series of GFP-tagged transgenes. Expression of PfHRPIIGFP in *P. falciparum*-infected erythrocytes produced a \approx 75-kDa tagged protein recognized by antibodies to GFP (Fig. 1*B* lane i) and PfHRPII (data not shown): The abundance of histidines leads to anomalous migration of the protein product (the predicted size is \approx 68 kDa). Over 90% of the GFP signal is due to PfHRPIIGFP. Removal of the histidine-rich domain amino acids 57–327 (resulting in the expression of SSHRPII-DomainIGFP) gave rise to low levels of a precursor (Fig. 1*B* lane ii, arrow) with most of the fusion protein processed to an expected, mature 33-kDa protein (Fig. 1*B* lane ii, arrowhead). In cells expressing SSGFP (a fusion of the ER-type SS and GFP), low levels of the secretory precursor (Fig. 1*B* lane iii, arrow) as well as mature GFP are detected (Fig. 1*B* lane iii, arrowhead). The presence of the precursors may reflect posttranslational recruitment to the parasite ER [components of posttranslational machinery have been reported in the plasmodial genome database (32)]. Alternatively, precursors may be detected because of overproduction of the transgene; whichever the case, they indicate secretory processing of the SS. Cells transfected with SSHRPIIDomainIHis.reg._{57–124}GFP or SSHRPIIDomainIHis.minGFP express fusion proteins of \approx 40 and \approx 35 kDa corresponding to the expected molecular mass (Fig. 1*B* lane iv and *B* lane v). A cytosolic GFP-histidine protein chimera migrated anomalously at \approx 70 kDa instead of 45 kDa (Fig. 1*B* lane vi, again presumably because of the high proportion of histidine-rich sequence). When this chimera is placed downstream of secretory GFP, as in SSGFPHis.reg._{154–327}, a processed secretory fusion protein band of \approx 70 kDa was expressed (Fig. 1*B* lane vii).

To dissect the transport signals resident in PfHRPII, we examined the distribution of these GFP-tagged proteins by high-resolution fluorescence microscopy. As shown in Fig. 2*Ai*, green fluorescence caused by PfHRPIIGFP (which represents 90% of the GFP signal) is detected over the parasite (p), tubovesicular membranes extending from the parasite (arrow), and erythrocyte (e) in live cells. One possible reason for the prominent parasite-associated green fluorescence is that the *cam* promoter used to drive the transgene is constitutive and active in the rings and trophozoites [i.e., from 0 to 36 h of intraerythrocytic infection (18)], resulting in continuous production of PfHRPIIGFP at these stages. We have shown previously that as much as 97% of the endogenous PfHRPII protein is detected in the red cell by the trophozoite stage (18). However, the endogenous *hrpII* promoter is active only in the earlier ring-stage parasites (0–16 h of infection) and no longer active at the trophozoite stage. [Note that, unlike targeting to the apical organelles, export to the erythrocyte cytosol occurs at all stages of intracellular parasite growth (18).]

Treatment with tetanolysin (33) (a toxin that selectively lyses the red cell but not the vacuolar or parasite plasma membrane) followed by Western blotting of pellet and supernatant fractions (Fig. 2*B*, lanes 1 and 2) revealed that 40% of PfHRPIIGFP is exported to the erythrocyte cytosol as determined by densitometry (data not shown). Removal of the histidine-rich domain (amino acids 57–327) abrogated export of green fluorescence to the erythrocyte cytoplasm (Fig. 2*Aii*). However, in 90% of infected cells, intraerythrocytic tubules and loops emerging from the parasite continue to be labeled (marked with an arrow in Fig. 2*Aii* and Movie 1, which is published as supporting information on the PNAS web site). Tetanolysin treatment (Fig. 2*B*, lanes 3 and 4) confirmed that failure to detect erythrocytic green fluorescence was due to a block in the export of DomainIGFP into the erythrocyte cytosol rather than its degradation into nonfluorescent fragments. Further, the ER-type SS (amino acids 1–27) delivered GFP to periphery of the parasite and associated intraerythrocytic loops (marked with an arrow in Fig. 2*Aiii* and seen in >50% of infected cells), consistent with transport to the

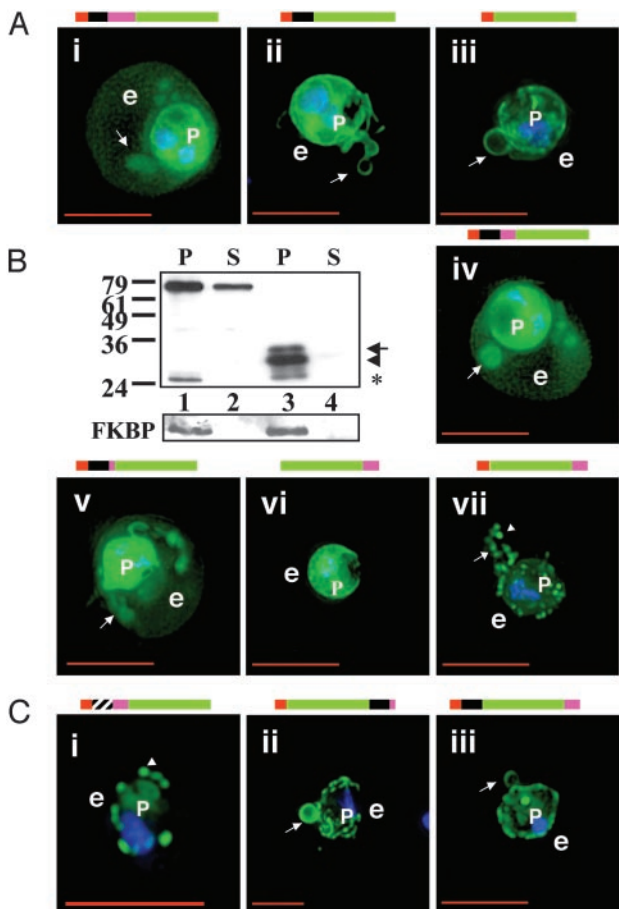


Fig. 2. Identification and characterization of a VTS in *P. falciparum*-infected erythrocytes. (A) Projections (0°) of live cells expressing PfHRPIIGFP (i), SSHRPIIDomainIGFP (ii), SSGFP (iii), SSHRPIIDomainIHis.reg.57–124GFP (iv), SSHRPIIDomainIHis.min.GFP (v), GFPHis.Reg.154–327 (vi), and SSGFPHis.reg.154–327 (vii). Green, GFP; blue, nuclei; p, parasite; arrow, vacuolar tubules and loops; arrowhead, punctate spot; e, erythrocyte. In GFP fusions: orange, the SS; black, domain I; hatched region, deleted domain I (Δ Domain I) construct (see *Materials and Methods*); pink, histidine-rich regions (of differing lengths; domain II); green, GFP. A minimal (9-aa) histidine-rich sequence (containing four histidines) from the histidine domain II downstream of domain I is essential for vacuolar export of GFP to the erythrocyte cytoplasm. (B) Western blots of supernatant (S) and pellet (P) fractions after tetanolysin treatment of cells (see *Materials and Methods*) expressing PfHRPIIGFP (lanes 1 and 2) and SSDomainIGFP (lanes 3 and 4). PFKBP in the plasmodial cytoplasm was used to confirm parasite integrity (the antibody was a kind gift of T. Wandless, Stanford University, Stanford, CA). (C) Live cells expressing SSHRPIIDomainIHis.reg.57–124 GFP (i), SSGFPHis.reg.154–327 (ii), and SSHRPIIDomainIGFPHis.reg.154–327 (iii). Domain I seems to be required along with the minimum histidine sequence to form a VTS. Further, DomainIHis.min must be contiguous and immediately downstream of SS to mediate protein export from the PV to the erythrocyte cytoplasm. (Scale bar, 5 μ m.)

PV (8). These data suggest that the SS of PfHRPII is sufficient to deliver GFP to vacuolar intraerythrocytic membranes. The presence of domain I may increase the frequency with which green fluorescence is detected in intraerythrocytic loops and tubules, but the terminal histidine-rich sequences are needed for significant export to the erythrocyte cytoplasm.

To investigate its transport properties further, the histidine region was truncated by approximately two-thirds to create SSDomainIHis.57–124GFP (Fig. 1) or replaced with a short 9-aa histidine-rich sequence VHHAHHADV, which approximates a minimal histidine repeat unit in PfHRPII to create SSDomainIHis.min.GFP. Both SSDomainIHis.reg.57–124GFP or SSDo-

mainIHis.minGFP were exported to the erythrocyte (Fig. 2*Avi* and *Av*), suggesting that the general property of histidine richness conserved throughout the C-terminal domain could reconstitute export.

In the absence of an SS, histidine-rich sequences failed to mediate protein export from the parasite (Fig. 2*Avi*). However, when placed downstream of secretory GFP, as in SSGFPHis.reg.154–327 (Fig. 1*Bvii*), histidine sequences targeted the reporter to punctate spots in the red cell (arrowheads in Fig. 2*Avii*). The spots and lesser-labeled tubules are clearly seen in Movie 2, which is published as supporting information on the PNAS web site. However, no green fluorescence was seen in the cytoplasm of the erythrocyte. This suggests that histidine-rich sequences alone export GFP from the PV to intraerythrocytic structures and possibly concentrate GFP in a subset of these membranes, but export to the erythrocyte cytoplasm requires domain I and histidine sequences. Hence, the domain I-histidine-rich chimera constitutes a VTS. A minimal histidine sequence downstream of the domain I region gives rise to a 38-aa peptidic VTS.

Deletion of domain I sequences (NLCSKNAKGLNL) abolishes export of green fluorescence to the erythrocyte cytosol, but GFP is detected in punctate spots proximal to the vacuolar parasite (see arrowhead in Fig. 2*Ci*). The placement of the VTS downstream of GFP or separation of the domain I and histidine-rich regions by GFP also results in loss of green fluorescence in the erythrocyte cytosol (Fig. 2*Cii* and *Ciii*), although loops emerging from the parasite continue to be labeled. The paucity of multiple, distinct markers in intraerythrocytic membranes makes it difficult to resolve whether these loops are equivalent to those shown in Fig. 2*Aii* and *Aiii*. Similarly, the relationship of punctate spots seen in Fig. 2*Ci* and *Avii* remain undefined. Nonetheless, the data in Fig. 2*C* confirm the importance of domain I as well as the requirement for contiguous domain I and histidine-rich sequences to cooperatively assemble the VTS.

The Histidine-Rich Domain Within the VTS Exports GFP Directly from the PV to the Maurer's Clefts. Our results from Fig. 2 suggest that, although histidine-rich sequences (of the VTS) alone cannot mediate the release of GFP to the erythrocyte cytosol, they can export protein to punctate spots connected by tubules and loops that emerge from the vacuole and extend into the intraerythrocytic region. Many parasite proteins exported to the red cell have been localized to intraerythrocytic structures called the Maurer's clefts (22–24), which may be attached to the erythrocyte cytoskeleton and appear as punctate spots by fluorescence microscopy (31, 34). Indirect immunofluorescence assays show that punctate intraerythrocytic “spots” targeted by histidine-rich sequences colocalize to a high degree with a resident protein of the clefts (31) at both early (ring, data not shown) and later (trophozoite) stages of parasite growth (Fig. 3*A–C* and enlarged area in 3*C'*). The presence of GFP in clefts in these cells was confirmed further by immunoelectron microscopy (see Fig. 5, which is published as supporting information on the PNAS web site). Short tubular and vesicular elements (see arrows in Fig. 3*C'*) may deliver GFP from the vacuolar parasite (p) to clefts (arrowheads in Fig. 3*C'*) as well as between adjacent clefts. In a cell showing 30 clefts in Fig. 3*A–C*, four to five are not labeled with green fluorescence; this could be due to reduced transit of GFP to peripheral clefts. In addition, a few areas of intraerythrocytic GFP do not colocalize with clefts, possibly because they represent transport intermediates. However, some of these may still connect clefts to each other as well as the vacuole. The VHHAHHADV sequence also delivers GFP to punctate intraerythrocytic structures (data not shown) at or proximal to clefts. Because with these constructs we fail to detect GFP in the erythrocyte cytoplasm in either live or fixed cells by using fluorescence and electron microscopy (Figs. 2, 3*A–C*, and 5*C* and *D*), it is possible that the histidine domain with the VTS may

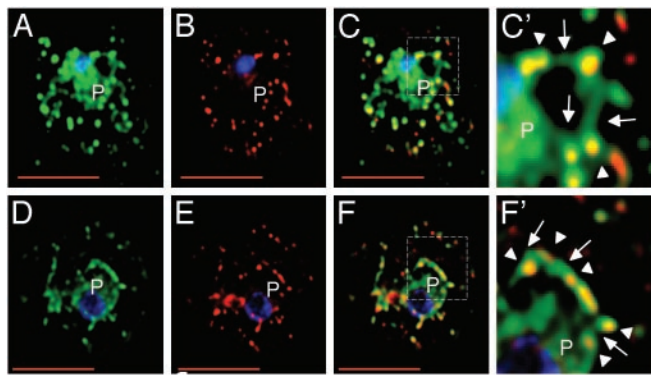


Fig. 3. The Maurer's clefts are intermediates in PfHRPII transport and are targeted by its histidine-rich sequences. Single optical sections of trophozoite-infected cells expressing SSGFPHis_{154–327} (A–C) or PfHRPIIGFP (D–F) are shown. Cells were fixed, permeabilized, subjected to indirect immunofluorescence assays (see *Materials and Methods*), and probed with antibodies to GFP (green) and a Maurer's cleft resident protein PfSBP (red). Magnification of the boxes in C and F are shown as C' and F', respectively. The extent of colocalization is shown in yellow. In C' and F', arrows indicate GFP-labeled tubules or vesicles connecting clefts to each other or the vacuolar parasite (P). Nuclei were stained with Hoechst (blue). (Scale bar, 5 μ m.)

mediate a direct route of export from the PV to clefts and tubovesicular structures proximal to them without transit through the erythrocyte cytosol.

We next were interested in determining whether GFP transgenes exported into the red cell cytoplasm could be detected in intraerythrocytic membranes such as those seen in Fig. 3 A–C. To do this, trophozoite stage-infected cells were fixed under conditions that remove hemoglobin and GFP in the erythrocyte cytoplasm and facilitate detection of GFP within intraerythrocytic structures. Subsequent indirect immunofluorescence assays (Fig. 3 D–F) reveal that PfHRPIIGFP fusions, as well as truncated forms that are exported to the red cell (data not shown), can also be detected in close association with Maurer's clefts (arrowheads in the enlargement shown in Fig. 3 F'), and lower levels of the transgene are seen in tubovesicular structures (arrows in Fig. 3 F') that appear to connect clefts to each other and vacuolar parasite. These data suggest that HRPIIGFP transgenes that are delivered to the erythrocyte cytoplasm may traffic through intraerythrocytic clefts. Further, in conjunction with the results shown in Figs. 2*Avii* and 3 A–C, it is possible that the route of PfHRPIIGFP export is mediated by transport properties of the histidine-rich domain within the VTS.

Chimeras of HRPI/HRPII Domain I and Histidine-Rich Domains (II) Reconstitute Functional VTS. In attempting to define a minimal VTS in other parasite proteins, we found that a secretory construct containing SS of PfHRPII and domain I of PfHRPI targeted GFP to the PV and associated tubules and loops (Fig. 4A). Addition of the minimal histidine region of PfHRPII (VHHAHHADV) downstream of the HRPIIDomainI restored export of green fluorescence to the erythrocyte cytoplasm (Fig. 4B). The addition of a polyhistidine sequence (containing 13 histidines) that resembles the first histidine-rich region of PfHRPI (35) downstream of the HRPIIDomainI also exported green fluorescence to the red cell (Fig. 4C). This strongly suggests that functionally equivalent, bipartite VTS signals are present in PfHRPI and PfHRPII. Remarkably, replacement of histidine (pKa of 6.5) with arginine (pKa of 12) in VHHAHHADV to produce VRRARRADV maintained export of GFP to the red cell (Fig. 4D). [Note that intraerythrocytic structures are labeled in Fig. 4 B–D (data not shown).] Hence, there may be a need for basic, positively charged amino acids in the VTS,

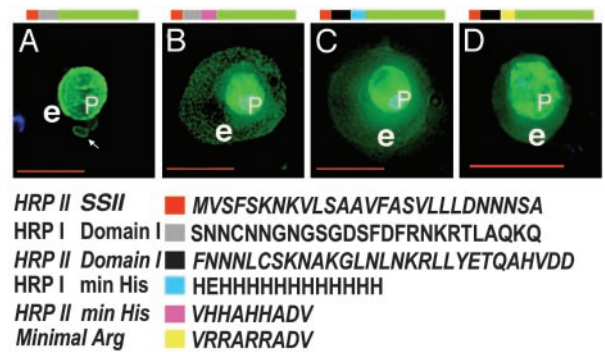


Fig. 4. Functionally equivalent bipartite VTS from PfHRPI/PfHRPII and histidine-to-arginine substitutions. Note that, in chimeric VTS, HRPI sequences are shown in bold type, and HRPII sequences are shown in bold and italic type. Live cells expressing SSHRPIDomainIGFP (A), SSHRPIDomainIHRPIHis.min.GFP (B), SSHRPIDomainIHRPIHis.min.GFP (C), and SSHRPIDomainIArg.min.GFP (D) are shown. DNA was visualized by Hoechst stain (blue). e, erythrocyte; p, parasite. The color code shows indicated regions in each chimera. Domain I and minimal histidine sequences from domain II of HRPI and HRPII are interchangeable in a VTS. Arginine can substitute for histidine in a VTS. (Scale bar, 5 μ m.)

and this may be fulfilled by histidine if the vacuole and/or clefts are even mildly acidic. The presence of histidines in HRPs may reflect a strategy to be charged in transport but neutral in the red cell.

Discussion

Although solutes in the vacuole and attached intraerythrocytic membranes are thought to access the erythrocyte cytosol by a nonspecific pore (36), our data here show that protein movement out of the vacuole to the red cell is regulated by a bipartite VTS. Previous studies (24) concluded that domain I of PfHRPI was insufficient to export a GFP transgene from the PV to the red cell and failed to recognize the contribution of this region to the VTS. Rather, they proposed that a “translocation motif” that resided in non-histidine-rich sequences of the histidine-rich domain was important for release to the erythrocyte (24). Here we show that a vacuolar translocation motif resides in domain I and minimal histidine-rich sequences (of domain II) derived from PfHRPII and equivalent signals reside in PfHRPI, suggesting that these motifs constitute a malarial VTS.

Eukaryotic pathogens that are extracellular secrete virulence determinants to their surface via an ER-type SS (37, 38). However, those that reside intracellularly need an additional vacuolar export signal to be delivered to the host cytoplasm. The malarial VTS described in this study is a defined export signal for a eukaryotic, vacuolar pathogen. VTSs are recognized as virulence secretion signals in prokaryotes (39, 40) and viruses (41). Further, positively charged, arginine-rich peptides have been shown to provide the membrane translocation signals in the prokaryotic twin arginine transport (TaT) system (40), TAT sequence of HIV, and antennapedia peptides (41). The malarial VTS may be positively charged, but database analyses failed to reveal conserved machinery required for TaT-mediated transport in *P. falciparum*. Moreover, TAT and antennapedia peptide sequences from HIV and *Drosophila* enable translocation across most eukaryotic cell membranes and are likely to act independently of transporters by directly destabilizing lipid organization in the bilayer. In contrast, the malarial VTS does not mediate export across the erythrocyte membrane (18), and translocation across the cleft membrane requires domain I in addition to the histidine/arginine domain. In this regard, the malarial VTS presents a unique membrane transport/translocation signal in eukaryotic cells (42).

Wickham *et al.* (24) proposed that PfHRPI is translocated across the PV into the erythrocyte cytoplasm and subsequently transported to the cytoplasmic face of Maurer's clefts (where it assembles into a cytoadherence complex with PfEMP1) and finally the erythrocyte membrane. However, this model was developed in the absence of defining the critical transport signals needed for protein delivery into the erythrocyte cytosol, Maurer's clefts, or other intraerythrocytic membranes. In addition, there was no quantitative evidence presented that protein release from the PV into the erythrocyte cytosol precedes transport from PV to clefts. Finally, because PfEMP1 is exported to the surface of infected erythrocyte lacking PfHRPI, there is no compelling argument that recruitment of soluble HRPI on the cytoplasmic face of Maurer's clefts is required for the export of PfEMP1 *per se*. Our data show that PfHRPII and PfHRPI contain equivalent VTSs and thus are likely to use the same transport apparatus in export from the vacuole to the erythrocyte cytoplasm. Further we show that, in live cells, histidine-rich sequences target GFP from the PV to the Maurer's clefts via tubules and vesicles and without release into the erythrocyte cytosol. Thus, it is possible that VTS-mediated exit to the cytoplasmic face of the erythrocyte may occur at clefts rather than the PV. Because clefts are thought to be proximal to the erythrocyte membrane, this may explain why, in addition to the PfHRPI, PfHRPII is enriched at the periphery of the erythrocyte (18), and this may facilitate its interactions with the host cytoskeleton (17). Further studies are required to distinguish

between vacuolar intraerythrocytic sites of exit for histidine-rich and other proteins and whether tubovesicular intermediates that mediate export of GFP transgenes are the same or distinct from a network of nutrient import that we have shown previously exists in infected red cells (43).

Because most proteins are translated on cytosolic ribosomes, cells have developed complex transport machineries of cotranslational and posttranslational import into the secretory pathway and organelles such as the mitochondrion and peroxisomes (42). Proteins recruited into the secretory pathway or other subcellular organelles remain there without exiting into the cytoplasm of the cell. In contrast, malarial vacuolar intraerythrocytic structures seem to be specialized eukaryotic organelles with dedicated parasite-encoded transporters that catalyze exit of secretory proteins into the cytoplasm. The VTS-intraerythrocytic cleft system seems to be prominent in the unusual biological niche that arises at this host-pathogen interface. Importantly, the signal recognized by this transport system is unique, and thus it may be possible to identify compounds that block interactions of the VTS with no detriment to organellar translocation functions in the mammalian host.

We thank Dr. Dianne Taylor for antibody to PfHRPII and Dr. N. Cianciotto, N. L. Hiller, and C. Olson for careful reading of the text. This work was supported by National Institutes of Health Grants AI26670 and HL69630 and a New Initiatives in Malaria Award from the Burroughs Wellcome Fund (to K.H.).

1. Chasis, J. A., Prenant, M., Leung, A. & Mohandas, N. (1989) *Blood* **74**, 1112–1120.
2. Schrier, S. L. (1985) *Clin. Haematol.* **14**, 1–12.
3. Gratzler, W. R. & Dluzewski, A. R. (1993) *Semin. Hematol.* **30**, 232–247.
4. Holder, A. A., Guevara Patino, J. A., Uthaiipibull, C., Syed, S. E., Ling, I. T., Scott-Finnigan, T. & Blackman, M. J. (1999) *Parassitologia (Rome)* **41**, 409–414.
5. World Health Organization (2002) *Roll Back Malaria Information Sheet* (World Health Organization, Geneva).
6. Miller, L. H., Baruch, D. I., Marsh, K. & Doumbo, O. K. (2002) *Nature* **415**, 673–679.
7. Deitsch, K. W. & Wellems, T. E. (1996) *Mol. Biochem. Parasitol.* **76**, 1–10.
8. Haldar, K., Mohandas, N., Samuel, B. U., Harrison, T., Hiller, N. L., Akompong, T. & Cheresch, P. (2002) *Cell. Microbiol.* **4**, 383–395.
9. Kilejian, A., Sharma, Y. D., Karoui, H. & Naslund, L. (1986) *Proc. Natl. Acad. Sci. USA* **83**, 7938–7941.
10. Panton, L. J., McPhie, P., Maloy, L. W., Wellems, T. E., Taylor, D. W. & Howard, R. J. (1989) *Mol. Biochem. Parasitol.* **35**, 149–160.
11. Oh, S. S., Chishti, A. H., Palek, J. & Liu, S. C. (1997) *Curr. Opin. Hematol.* **4**, 148–154.
12. Sullivan, D. J., Jr., Gluzman, I. Y. & Goldberg, D. E. (1996) *Science* **271**, 219–222.
13. Choi, C. Y., Cerda, J. F., Chu, H. A., Babcock, G. T. & Marletta, M. A. (1999) *Biochemistry* **38**, 16916–16924.
14. Scorza, T., Magez, S., Brys, L. & De Baetselier, P. (1999) *Parasite Immunol. (Oxf.)* **21**, 545–554.
15. Sullivan, D. J., Jr., Matile, H., Ridley, R. G. & Goldberg, D. E. (1998) *J. Biol. Chem.* **273**, 31103–31107.
16. Taramelli, D., Monti, D., Omodeo-Sale, F., Basilio, N., Parapini, S., Pasini, E., Lomardi, L. & Olliaro, O. (2001) *Parassitologia (Rome)* **43**, Suppl. 1, 45–49.
17. Benedetti, C. E., Kobarg, J., Pertinhez, T. A., Gatti, R. M., Souza, O. N., Spisni, A. & Meneghini, R. (2003) *Mol. Biochem. Parasitol.* **128**, 157–166.
18. Akompong, T., Kadekoppala, M., Harrison, T., Oksman, A., Goldberg, D. E., Fujioka, H., Samuel, B. U., Sullivan, D. & Haldar, K. (2002) *J. Biol. Chem.* **277**, 28923–28933.
19. Albano, F. R., Berman, A., La Greca, N., Hibbs, A. R., Wickham, M., Foley, M. & Tilley, L. (1999) *Eur. J. Cell Biol.* **78**, 453–462.
20. Adisa, A., Albano, F. R., Reeder, J., Foley, M. & Tilley, L. (2001) *J. Cell Sci.* **114**, 3377–3386.
21. Hayashi, M., Taniguchi, S., Ishizuka, Y., Kim, H. S., Wataya, Y., Yamamoto, A. & Moriyama, Y. (2001) *J. Biol. Chem.* **276**, 15249–15255.
22. Hinterberg, K., Scherf, A., Gysin, G., Toyoshima, T., Aikawa, M., Mazie, J. C., da Silva, L. P. & Mattei, D. (1994) *Exp. Parasitol.* **79**, 279–291.
23. Stanley, H. A., Langreth, S. G. & Reese, R. T. (1989) *Mol. Biochem. Parasitol.* **36**, 139–150.
24. Wickham, M. E., Rug, M., Ralph, S. A., Klonis, N., McFadden, G. I., Tilley, L. & Cowman, A. F. (2001) *EMBO J.* **20**, 5636–5649.
25. Cheresch, P., Harrison, T., Fujioka, H. & Haldar, K. (2002) *J. Biol. Chem.* **277**, 16265–16277.
26. Waller, R. F., Reed, M. B., Cowman, A. F. & McFadden, G. I. (2000) *EMBO J.* **19**, 1794–1802.
27. Adisa, A., Rug, M., Klonis, N., Foley, M., Cowman, A. F. & Tilley, L. (2003) *J. Biol. Chem.* **278**, 6532–6542.
28. Kadekoppala, M., Kline, K., Akompong, T. & Haldar, K. (2000) *Infect. Immun.* **68**, 2328–2332.
29. Fidock, D. A. & Wellems, T. E. (1997) *Proc. Natl. Acad. Sci. USA* **94**, 10931–10936.
30. Deitsch, K., Driskill, C. & Wellems, T. (2001) *Nucleic Acids Res.* **29**, 850–853.
31. Li, W.-I., Das, A., Song, J.-Y., Crary, J. L. & Haldar, K. (1991) *Mol. Biochem. Parasitol.* **49**, 157–168.
32. Gardner, M. J., Hall, N., Fung, E., White, O., Berriman, M., Hyman, R. W., Carlton, J. M., Pain, A., Nelson, K. E., Bowman, S., *et al.* (2002) *Nature* **419**, 498–511.
33. Riese, M. J., Goehring, U. M., Ehrmantraut, M. E., Moss, J., Barbieri, J. T., Aktories, K. & Schmidt, G. (2002) *J. Biol. Chem.* **277**, 12082–12088.
34. Blisnick, T., Morales Betoulle, M. E., Barale, J. C., Uzureau, P., Berry, L., Desroses, S., Fujioka, H., Mattei, D. & Braun Breton, C. (2000) *Mol. Biochem. Parasitol.* **111**, 107–121.
35. Pologe, L. G. & Ravetch, J. V. (1986) *Nature* **322**, 474–477.
36. Desai, S. A., Krogstad, D. J. & McCleskey, E. W. (1993) *Nature* **362**, 643–646.
37. Lee, S. A., Mao, Y., Zhang, Z. & Wong, B. (2001) *Microbiology* **147**, 1961–1970.
38. Arioka, M., Hirata, A., Takatsuki, A. & Yamasaki, M. (1991) *J. Gen. Microbiol.* **137**, 1253–1262.
39. Miao, E. A. & Miller, S. I. (2000) *Proc. Natl. Acad. Sci. USA* **97**, 7539–7544.
40. Ochsner, U. A., Snyder, A., Vasil, A. I. & Vasil, M. L. (2002) *Proc. Natl. Acad. Sci. USA* **99**, 8312–8317.
41. Futaki, S., Nakase, I., Suzuki, T., Youjun, Z. & Sugiura, Y. (2002) *Biochemistry* **41**, 7925–7930.
42. Schatz, G. & Dobberstein, B. (1996) *Science* **271**, 1519–1526.
43. Lauer, S. A., Rathod, P. K., Ghori, N. & Haldar, K. (1997) *Science* **276**, 1122–1125.
44. Wellems, T. E. & Howard, R. J. (1986) *Proc. Natl. Acad. Sci. USA* **83**, 6065–6069.